and L. K. Galbraith for their essential contributions in designing and building the equipment. One of us (P.E.V.) would like to thank the Council for Scientific and Industrial Research and the University of the Orange Free State, Republic of South Africa, for travel support, and Yale University for its hospitality.

*Work supported by the Night Vision Laboratory, Fort Belvoir, Virginia, under Contract No. DAAK 022-68-C-0232, and by the National Science Foundation Institutional Grant No. GU-1658.

†On leave from the University of the Orange Free State, Bloemfontein, Republic of South Africa.

[1]See for example, G. Heiland and L. Lamatsch, Surface Sci. 2, 18 (1964); and D. R. Palmer, S. R. Morrison, and C. E. Dauenbaugh, Phys. Rev. Lett. 6, 170 (1961); also, G. Busch and T. E. Fischer, Phys. Kondens. Mater. 1, 367 (1963).

[2]A. Y. Cho and J. R. Arthur, Jr., Phys. Rev. Lett. 22, 1180 (1969).

[3]J. H. Dinan, L. K. Galbraith, and T. E. Fischer, to be published.

[4]F. G. Allen and G. W. Gobeli, Phys. Rev. 127, 150 (1962).

[5]J. R. Smith, Phys. Rev. Lett. 25, 1023 (1970).

[6]C. G. B. Garrett and W. H. Brattain, Phys. Rev. 99, 376 (1955).

[7]T. E. Fischer, Surface Sci. 13, 31 (1969).

[8]P. E. Viljoen and T. E. Fischer, to be published.

[9]G. W. Gobeli and F. G. Allen, Phys. Rev. 137, A246 (1965).

[10]J. Wojas, Phys. Status Solidi 35, 903 (1969).

[11]J. Rowe, in *Proceedings of the Tenth International Conference on the Physics of Semiconductors, Cambridge, Mass., 1970,* edited by S. P. Keller, J. C. Hensel, and F. Stern, CONF-700801 (U.S. AEC Division of Technical Information, Springfield, Va., 1970), p. 217.

Carrier Transport and Potential Distributions for a Semiconductor *p-n* Junction in the Relaxation Regime

H. J. Queisser,* H. C. Casey, Jr., and W. van Roosbroeck
Bell Telephone Laboratories, Murray Hill, New Jersey 07974
(Received 21 December 1970)

Experimental current-voltage characteristics and potential distributions are presented for a *p-n* junction in high-resistivity GaAs, whose dielectric relaxation time τ_D exceeds carrier lifetime τ_0. The condition $\tau_D > \tau_0$ defines the new "relaxation regime" for which theory predicts behavior entirely different from that of the familiar ideal rectifier of conventional semiconductor physics with $\tau_D \ll \tau_0$. The predicted field distributions and the linear and sublinear current-voltage relationships are observed. These results confirm the theory in detail.

A new semiconductor regime is realized when the dielectric relaxation time $\tau_D = \rho\epsilon$ exceeds the carrier diffusion-length lifetime τ_0.[1-3] This "relaxation-case" regime can be obtained in crystalline or amorphous semiconductors doped with deep traps, which raise the resistivity ρ and shorten the lifetime τ_0. We call the conventional semiconductor behavior the "lifetime case," since $\tau_0 \gg \tau_D$ is always assumed.[4]

Departures from local neutrality are predicted for the relaxation case,[1-3,5] and a small-signal injected neutral pulse drifts in the majority-carrier direction.[1,5] In addition, the net local recombination rate is approximately zero after an initial rapid recombination.[1-3] The injected minority carriers can both reduce the majority-carrier concentration and fill ionized traps.[2,3] Injected minority carriers thus *increase* resistivity because of this recombinative depletion. "Lifetime-case" injection, of course, *reduces* resistivity.[4]

This paper describes current-voltage and potential-distribution measurements for GaAs *p-n* junctions which illustrate and confirm the theory of the relaxation regime. The current-voltage dependence of a relaxation-case junction is found to be completely different from the well-known "ideal-rectifier" junction with its exponentially increasing forward current and saturated reverse current.[6]

Oxygen-doped and compensated single crystals of n-type GaAs with $n_0 = 3\times10^7$ electrons/cm^3 and mobility $\mu_n = 4.5\times10^3$ cm^2/V sec were used. Zinc diffusion created a 3×10^{-4}-cm deep p layer with $p_s > 10^{20}$ holes/cm^3 at the surface. Ohmic In-Au contacts were evaporated and alloyed. The volume resistivity after these treatments was found by potential probing (in region "1*f*" of Fig. 1) to be $\rho = 1.5\times10^8$ Ω cm at 22°C. With ϵ(GaAs) $\approx 10^{-12}$ F/cm, we get $\tau_D = \rho\epsilon \approx 10^{-4}$ sec $\gg \tau_0 \lesssim 10^{-8}$ sec.

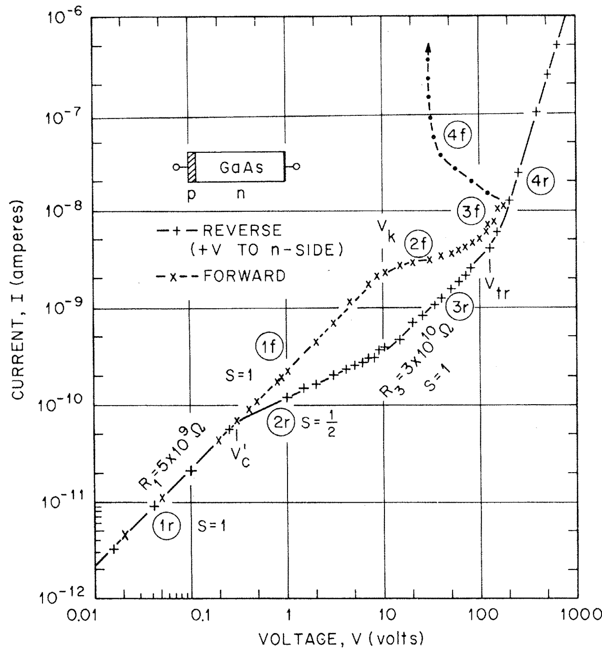

FIG. 1. Logarithmic plot of current-voltage characteristics for a GaAs p-n junction in the relaxation regime. Temperature 22°C, diode measured in darkness. The solid line is for reverse bias, positive voltage to the n region. The dashed line is for forward bias. Regions "$1r$" to "$4f$" with indicated slopes $S \equiv d\ln I/d\ln V$ are discussed in the text.

Results for diode No. 14 (area $A = 4\times10^{-3}$ cm^2, length $L = 4.5\times10^{-2}$ cm) are shown in Fig. 1. We discuss the distinct regions of the $I(V)$ curves individually, using simplified concepts here rather than large-signal nonlinear theory.[2,3]

Reverse-bias region "$1r$", $|V| < 0.2$, is linear ($S = d\ln I/d\ln V = 1$) corresponding to $R_1 = 5\times10^9\ \Omega$. The resistance R_1 is about three times greater than expected from the n region alone. The largest contribution to R_1 is by the space-charge region (SCR) adjacent to the junction. The positive charge is fixed at donors and traps. The SCR width $w = 7\times10^{-3}$ cm was obtained by capacitance measurements[7] and by potential probing. Average resistivity in the SCR is thus $\rho = 2\times10^9\ \Omega$ cm, close to the "maximum resistivity,"[2,3]

$$\rho_{\max} = b^{1/2}/2qn_i\mu_n, \tag{1}$$

where b is the mobility ratio μ_n/μ_p, q is the electron charge, and n_i is the intrinsic carrier concentration. The maximum resistivity is a significant quantity in relaxation-case material. The condition $\tau_D > \tau_0$ implies a region of steady-state zero local recombination,[1] which in turn requires that the product of the steady-state hole and electron concentrations n and p is constant:

$$np = n_i^2 \neq n_i^2 \exp(qV/kT). \tag{2}$$

Here the last expression is essential in the conventional lifetime regime.[4,6] Equation (1) implies $n(\rho_{\max}) = n_m = n_i b^{-1/2}$, $p_m = n_i b^{1/2}$, and $\mu_n n_m = \mu_p p_m$. Resistivity in an SCR can be shown to approach $\rho_{\max}$ in the relaxation case.[8] At 22°C, $n_i = 9\times10^5$ carriers/cm^3,[9] $b \approx 20$,[10] and thus $\rho_{\max} \approx 3\times10^9\ \Omega$ cm.

Reverse currents are sustained by carriers thermally generated in the SCR. Sufficiently low reverse voltages do not deplete electrons near the interface of the SCR and n region, because electrons can diffuse back. A measure of this diffusion tendency is the equilibrium contact potential between the SCR and n region, which can be expressed by

$$V_c = (kT/q)[\ln(n_0/n_m)] \approx 0.1\ \text{V}. \tag{3}$$

When reverse bias (V_c' of Fig. 1) becomes comparable to V_c plus the IR drop in the n region, the SCR widens by Δw through removal of mobile electrons. Incremental resistance ΔR and current ΔI are both proportional to Δw, thus

$$\Delta I \propto \Delta R = \Delta V/\Delta I, \quad \Delta I \propto (\Delta V)^{1/2}. \tag{4}$$

The sublinear region "$2r$" obeys the predicted onset involving the estimate of Eq. (3) and the square-root dependence $S = \frac{1}{2}$ of Eq. (4). Region "$2r$" should end when the entire sample is an SCR, which implies $R_3 = \rho_{\max} L/A \approx 3\times10^{10}\ \Omega$. This prediction that the linear region "$3r$" has resistance R_3 is verified.

Space-charge–limited currents constitute region "$4r$." This mechanism is well understood from the work of Rose and Lampert.[11,12] Onset occurs at[12]

$$V_{\text{tr}} = \tfrac{8}{9} qpN_t^{\,p} L^2/\epsilon, \tag{5}$$

where $N_t^{\,p}$ is the ratio of trapped to free holes. From the experimental $V_{\text{tr}} \approx 120$ V for hole injection from the n-side contact, we deduce $pN_t^{\,p} \approx 4\times10^{11}$ holes/cm^3 and estimate $N_t^{\,p} \approx 10^5$, using $p = p_m$. The well-known V^2 law,[12]

$$I = (\tfrac{9}{8} A\epsilon\mu_p/L^3 N_t^{\,p})V^2, \tag{6}$$

is usually observed throughout "$4r$." Often, as in Fig. 1, the V^2 law is followed by a steeper increase ($S \approx 3$) which might be the $I \propto V^3$ law of Lampert and Rose in their "low-field approximation"[12,13] of double injection.

Forward branch "$1f$" extends linearly to about 10 V, while linearity in the lifetime case ends at

$V=kT/q\approx 2.5\times 10^{-2}$ V at 300°K. The SCR resistance R_1 dominates as in "1r." Holes and electrons are swept into the SCR where rapid recombination insures Eq. (2). The sublinear region "2f" with $S\approx 0.4$ begins when injected holes traverse the entire SCR width w. These holes deplete majority electrons and widen the SCR, increasing resistance. Space charge is built up through hole capture by Coulomb-attractive centers, which become neutral and no longer compensate the positive donors. Detailed theory is complicated,[3] but a simple estimate of the kink voltage V_k can be made by neglecting diffusion. The average field V_k/w must suffice for traversal of w within a lifetime τ_p, yielding

$$V_k = w^2/\mu_p\tau_p; \tag{7}$$

see Refs. 12 and 13 for a similar argument in a different regime. The experimental $V_k\approx 10$ V implies $\tau_p\approx 2\times 10^{-8}$ sec (with $\mu_p = 2\times 10^2$ cm^2/V sec), which seems not too long a lifetime since most hole traps are now filled. Region "3f" is not pronounced and believed to be space-charge limited.[11-13] Region "4f," shown schematically by the dash-dotted curve, illustrates the negative resistance of double injection.[12,13]

The potential plots of Fig. 2 verify our interpretations. Curve A is typical for region "1f" with its SCR and Ohmic n-type material. From curves B to F (region "2f," Fig. 1), SCR widening with increasing bias is evident. The distinct ranges of electric field are exemplified in curve C. The region α is the high-field SCR, while β is a narrow layer of very low field, the predicted[3] "branch point," where the current is by hole diffusion. The adjacent high field of region γ produces drift of holes and electrons in a depleted layer, the "depletion drift region."[2,3] The region δ is adjacent to the "recombination front,"[2,3] and the field is much lower than in region ζ of the unmodulated material because n is much greater than n_0.[3] The potential profiles under reverse bias also agree with our interpretations. In region "2r" a "generation front" moves towards the n-region contact, while region "3r" has uniform high field and $\rho\approx\rho_{\max}$.

Temperature T affects the currents because of the exponential temperature dependence of n_i. We therefore measured $I(V)$ above room temperature. As expected, all linear and sublinear relaxation-case currents scale with the ratio $N \equiv n_i(T_1)/n_i(T_2)$. For example, at 54°C, n_i is 2.3 $\times 10^7$ cm^{-3}.[9] The transition voltages are merely reduced by 10%. The space-charge–limited currents in ranges "4r" and "3f," however, increase by only about 0.6N, which distinguishes them from the relaxation-case currents.

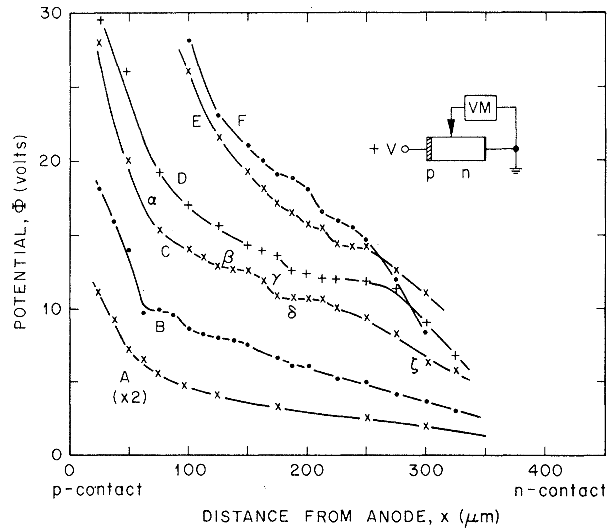

FIG. 2. Potential distributions for the junction of Fig. 1. The potential values were obtained with a 5 $\times 10^{-4}$-cm tungsten tip which was dragged across the diode. The voltmeter (VM) (see inset) had an input impedance of $\approx 10^{14}$ Ω and a maximum voltage range of 30 V. Temperature is 22°C. Curve A: 6 V total applied forward bias, $I = 1.4\times 10^{-9}$ A. Curve B is for 20 V total forward bias; C, 30 V; D, 40 V; E, 50 V; and F, 60 V. Greek letters signify typical ranges of electric field proportional to slopes of curves, as described in the text.

In conclusion, a p-n junction in a semiconductor with $\tau_D > \tau_0$ is completely different from the conventional lifetime-case ideal rectifier. The distinct regions of linear and sublinear $I(V)$ relations can be explained by the basic ideas of the theory of the relaxation regime. Large classes of crystalline and amorphous materials obey the relaxation-case condition. We expect wide variations in experimental $I(V)$ relations, because the parameters shown to be relevant, such as geometry, mobilities, trap densities, and lifetimes, can vary by orders of magnitude.

We wish to thank F. Ermanis for making the Hall measurements. D. A. Harrison assisted with the experiments. One of us (H.J.Q.) is particularly grateful for the hospitality extended to him by his friends and colleagues at Bell Telephone Laboratories during a most stimulating summer visit.

---

*Permanent address: Physikalisches Institut, Universität Frankfurt am Main, Frankfurt am Main, Germany.

[1]W. van Roosbroeck, Phys. Rev. 123, 474 (1961).

[2]W. van Roosbroeck and H. C. Casey, Jr., in *Proceedings of the Tenth International Conference on the Physics of Semiconductors, Cambridge, Mass., 1970*, CONF-700801, edited by S. P. Keller, J. C. Hensel, and F. Stern (U. S. AEC Division of Technical Information, Springfield, Va., 1970), p. 276.

[3]W. van Roosbroeck and H. C. Casey, Jr., to be published.

[4]W. Shockley, *Electrons and Holes in Semiconductors* (Van Nostrand, Princeton, N. J., 1950). In particular, see Chap. 3, pp. 58 and 59, for the significance of a finite minority-carrier lifetime for conductivity increase and a short relaxation time for neutrality.

[5]F. Stöckmann, in *Proceedings of the Photoconductivity Conference, Atlantic City, N. J., 1954*, edited by R. G. Breckenridge (Wiley, New York, 1956), p. 269.

[6]W. Shockley, Bell Syst. Tech. J. 28, 435 (1949), or any textbook on conventional semiconductor physics.

[7]We thank E. H. Nicollian for taking these data for us. The ac conductance and capacitance do not vary significantly up to 10^5 Hz with voltages <0.3 V peak to peak.

[8]See Ref. 3 for the exact conditions for $\rho \rightarrow \rho_{max}$. A simple argument at drift-only reverse bias is as follows: Carriers with the larger mobility-concentration product carry the larger fraction of current, and are thus more rapidly depleted until $\mu_n n = \mu_p p$ under the constraint $np = n_i^2$ of Eq. (2).

[9]H. C. Casey, Jr., and F. Ermanis, unpublished calculations of $n_i(T)$, including temperature dependence of energy gap.

[10]Estimate based on typical results; see, for example, S. Sze, *Physics of Semiconductor Devices* (Wiley, New York, 1969), Table 2.3, p. 58.

[11]A. Rose, Phys. Rev. 97, 1538 (1955).

[12]M. A. Lampert, Phys. Rev. 103, 1648 (1956), and Rep. Progr. Phys. 27, 329 (1964).

[13]M. A. Lampert, RCA Rev. 20, 682 (1959); M. A. Lampert and A. Rose, Phys. Rev. 121, 26 (1961).

Observation of Exciton Polariton Dispersion in CuCl†

D. Fröhlich,* E. Mohler, and P. Wiesner

Physikalisches Institut der Universität Frankfurt am Main, Frankfurt am Main, Germany

(Received 27 January 1971)

The upper branch of an exciton-polariton curve is measured directly for the first time. The two-photon spectrum of the first exciton line of CuCl shows a strong dependence on the total K vector of the two beams. The resulting dispersion curve can be quantitatively explained using one-photon data.

Polaritons result from the strong coupling between the polarization in a crystal and the electromagnetic radiation field.[1] They describe the normal modes of the coupled system. Depending on the mechanism of polarization, phonon and exciton polaritons are possible. Polaritons are already inherent in the solution of Maxwell's equations for a medium characterized by a dielectric constant, and thus are an intrinsic feature of classical crystal optics. In the quantum mechanical description of the optical dispersion and absorption process they provide a more detailed view in terms of elementary excitations.[2] As pointed out by Hopfield,[3] polaritons are a particularly useful concept when discussing experiments in which the polarization is driven by a weak coupling force different from the strong couplings already included in the polariton states. These kinds of interactions may arise in special situations of crystal optics,[4] in Raman scattering,[5] and in other fields of nonlinear optics including two-photon absorption.

The polariton effect in Raman scattering has become an especially useful tool for studying the dispersion relation of phonon polaritons.[6] In view of the close relationship between Raman and two-photon spectroscopy, the latter should be an equally suited method for measuring exciton-polariton dispersion. This measurement may be carried out by changing the angle between the two photon beams and thus tuning the wave vector of the excited polariton. It is the purpose of this Letter to present the first two-photon detection and dispersion measurement of the exciton polariton. We have chosen CuCl as the material since it is optically isotropic and possesses sharp $1s$-exciton lines which are clearly separated from the rest of the electronic spectrum.[7] Because of the lack of inversion symmetry in its point group (T_d), the polariton may be excited in the two-photon absorption process.

Two-photon spectra are measured with an automatic recording spectrometer[8] which provides an energy resolution of $\Delta E/E = 10^{-5}$. Figure 1 shows the experimental results in the neighborhood of the first exciton band of CuCl. In an unoriented crystal, two bands appear in this spectral region. The oscillator strengths and the energy separa-